



HAL
open science

Evolutionary processes and cellular functions underlying divergence in *Alexandrium minutum*

Mickael Le Gac, Gabriel Metegnier, Nicolas Chomérat, Pascale Malestroit, Julien Quéré, Olivier Bouchez, Raffaele Siano, Christophe Destombe, Laure Guillou, Annie Chapelle

► To cite this version:

Mickael Le Gac, Gabriel Metegnier, Nicolas Chomérat, Pascale Malestroit, Julien Quéré, et al.. Evolutionary processes and cellular functions underlying divergence in *Alexandrium minutum*. *Molecular Ecology*, 2016, 25 (20), pp.5129 - 5143. 10.1111/mec.13815 . hal-01400194

HAL Id: hal-01400194

<https://hal.sorbonne-universite.fr/hal-01400194v1>

Submitted on 21 Nov 2016

HAL is a multi-disciplinary open access archive for the deposit and dissemination of scientific research documents, whether they are published or not. The documents may come from teaching and research institutions in France or abroad, or from public or private research centers.

L'archive ouverte pluridisciplinaire **HAL**, est destinée au dépôt et à la diffusion de documents scientifiques de niveau recherche, publiés ou non, émanant des établissements d'enseignement et de recherche français ou étrangers, des laboratoires publics ou privés.

1 Original Article

2

3 **Evolutionary processes and cellular functions underlying divergence in**

4 ***Alexandrium minutum*.**

5

6 Mickael le Gac^{1*}, Gabriel Metegnier^{1,4}, Nicolas Chomérat², Pascale Malestroit¹, Julien Quéré¹, Olivier

7 Bouchez³, Raffaele Siano¹, Christophe Destombe⁴, Laure Guillou⁵, Annie Chapelle¹

8

9 ¹IFREMER, DYNECO/Pelagos, 29280 Plouzané, France

10 ²IFREMER, Station de Biologie Marine, 29900 Concarneau, France

11 ³GeT PlaGe, Genotoul, INRA Auzeville, Castanet Tolosan, France

12 ⁴Sorbonne Universités, Université Pierre et Marie Curie - Paris 6, CNRS, PUCCh, UACH, UMI 3614,
13 Evolutionary Biology and Ecology of Algae, Station Biologique de Roscoff, CS 90074, Place Georges
14 Teissier, CS90074, 29688 Roscoff cedex, France

15 ⁵Sorbonne Universités, Université Pierre et Marie Curie - Paris 6, CNRS, UMR 7144, Station
16 Biologique de Roscoff, Place Georges Teissier, CS90074, 29688 Roscoff cedex, France

17

18 Keywords : Speciation, Pseudocryptic species, Dinoflagellates, Harmful Algal Blooms, Populations
19 Genomics

20

21 *Corresponding author: Mickael Le Gac, Mickael.Le.Gac@ifremer.fr, Phone: (33)-298224358, Fax:
22 (33)-298224548.

23

24 Running Title: A. minutum divergence

25

26

27

28

29 Abstract

30 Understanding divergence in the highly dispersive and seemingly homogeneous pelagic environment
31 for organisms living as free drifters in the water column remains a challenge. Here, we analyzed the
32 transcriptome wide mRNA sequences, as well as the morphology of 18 strains of *Alexandrium*
33 *minutum*, a dinoflagellate responsible for Harmful Algal Blooms worldwide, to investigate the
34 functional bases of a divergence event. Analysis of the joint site frequency spectrum (JSFS) pointed
35 toward an ancestral divergence in complete isolations followed by a secondary contact resulting in
36 gene flow between the two diverging groups, but heterogeneous across sites. The sites displaying fixed
37 SNPs were associated with a highly restricted gene flow and a strong over-representation of non-
38 synonymous polymorphism, suggesting the importance of selective pressures as drivers of the
39 divergence. The most divergent transcripts were homologs to genes involved in calcium/potassium
40 fluxes across the membrane, calcium transduction signal and saxitoxin production. The implication of
41 these results in terms of ecological divergence and build-up of reproductive isolation are discussed.
42 Dinoflagellates are especially difficult to study in the field at the ecological level due to their small
43 size and the dynamic nature of their natural environment, but also at the genomic level due to their
44 huge and complex genome and the absence of closely related model organism. This study illustrates
45 the possibility to identify traits of primary importance in ecology and evolution starting from high
46 throughput sequencing data, even for such organisms.

47

48

49

50

51

52

53

54

55

56

57 Introduction

58 The high number of unicellular eukaryote species coexisting in an apparently homogeneous pelagic
59 environment has long puzzled ecologists (the paradox of the plankton, Hutchinson 1961). At the
60 ecological scale the paradox may be resolved, at least partly, by invoking out of equilibrium dynamics
61 (Roy and Chattopadhyay 2007). However, at the evolutionary scale the paradox remains extremely
62 puzzling. In the marine environment numerous species have a pelagic stage often associated with long
63 range dispersal creating high gene flow, opposing local adaptation and the speciation process (Palumbi
64 1992). For plants and animals with a benthic phase or animals able to swim against currents to remain
65 in specific habitats, adaptive divergence for specific environmental conditions seems nevertheless
66 possible (Bierne et al. 2003). For organisms remaining as free drifters in the water column, such as
67 phytoplankton, the forces that may drive such divergence are virtually unknown. Theoretical works
68 taking into account the huge population sizes, specific life history traits such as the ability to form
69 resting cysts embedded in the sediment, and the dependency on hydrodynamics not only as a
70 dispersive force of propagules but also as a force potentially impeding the organisms to remain in
71 favorable environmental conditions during active growth are extremely scarce (but see Shores et al.
72 2008). Empirically speaking, a growing number of population genetic studies have highlighted that
73 phytoplankton species may be spatially and temporally structured (Ryneckson et al. 2004; Iglesias-
74 Rodríguez et al. 2006; Masseret et al. 2009; Castelyn et al. 2010; Casabianca et al. 2012; Dia et al.
75 2014). Moreover, some works investigating ecological divergence between closely related species
76 have highlighted vertical niche partitioning in foraminifer (Weiner et al. 2012), specialization for
77 different light intensities and utilization of different parts of the light spectrum in cyanobacteria
78 (Rocap et al. 2003; Stomp et al. 2007), as well as divergence in term of metal usage in chlorophytes
79 (Palenik et al. 2007) and diatoms (Peers et al. 2006).

80 Dinoflagellates constitute an enigmatic group of mainly marine unicellular eukaryotes with lifestyles
81 ranging from mixotrophic (autotrophic and predator) to fully heterotrophic for half of the species,
82 sometimes producing toxins that have ecological, economic and sanitary impacts (Anderson et al.
83 2012a), and displaying many original genomic characteristics, including genome sizes among the
84 largest of any organisms (up to 60 times the size of the human genome, Wisecaver and Hackett 2011).

85 The species belonging to the genus *Alexandrium* (Anderson et al. 2012b) are responsible for paralytic
86 shellfish poisoning caused by the production of several toxins including saxitoxin (Cusick and Saylor
87 2013), a molecule classified as schedule 1 substance, in the sense of the Chemical Weapons
88 Convention due to its very low lethal dose.

89 Thanks to recent development in sequencing technologies and bioinformatics tools, it is now
90 becoming possible to investigate the genome-wide patterns of divergence (Seehausen et al. 2014).
91 These developments are not only transforming our understanding of divergence from an individual
92 gene to a whole genome perspective (Feder et al. 2013), but also enabling the investigation of genomic
93 divergence in a wide variety of organisms spanning the entire tree of life, including organisms that are
94 not closely related to any model organism (Ellegren 2014). So called reverse ecology approaches
95 where genomic data is the starting point to identify traits of ecological and evolutionary interest (Li et
96 al. 2008) are especially appealing for organisms that are difficult to study in the field, such as plankton
97 species, to gain insight on the evolutionary processes at play during divergence and the affected
98 cellular functions.

99 Here by sequencing and analyzing the mRNA sequences, as well as characterizing the morphology of
100 18 strains of *A. minutum* isolated from natural populations we highlight a divergence event. We
101 investigated: 1. The model of divergence most likely to explain the observed joint site frequency
102 spectrum among seven models of divergence, 2: Whether this event is driven by selective pressures,
103 and 3: What are the underlying divergent cellular functions.

104

105 Material and Methods

106 RNA extraction, library preparation and sequencing

107 Starting from environmental samples, each *A. minutum* strain was founded by micropipetting a single
108 cell into fresh medium under inverted microscope. Following isolation, the strains are maintained in
109 the lab by biweekly dilution into fresh media. Under culture conditions, cells are haploid and divide by
110 mitosis, each strain is thus composed of clonal individuals. A total of 18 strains isolated from various
111 localities and time (Fig. 1) were grown to mid exponential phase in 100 ml of K medium at 18°C,
112 12/12 photoperiod, and 80 $\mu\text{E}\cdot\text{s}^{-1}\cdot\text{m}^{-2}$ of irradiance. Cell densities ranged from $5\cdot 10^6$ to $2.5\cdot 10^7$ $\text{cell}\cdot\text{L}^{-1}$.

113 Cultures were centrifuged at 4,500 g for 8 min, sonicated on ice during 20 sec in RLT lysis buffer
114 (Qiagen) containing β -mercaptoethanol. Extraction was performed using RNeasy plus mini kit
115 (Qiagen) following the manufacturer protocol. Extracted RNA was quantified using a Biotek Epoch
116 spectrophotometer and the quality estimated on RNA 6000 nano chips using a Bioanalyzer (Agilent).
117 Reverse transcription of 4 μ g of total RNA into cDNA and library preparation were performed at the
118 GeT-PlaGe France Genomics sequencing platform (Toulouse, France) using the Illumina truseq RNA
119 V2 kits. One library was generated per *A. minutum* strain. Library quality was assessed on a
120 Bioanalyzer using high sensitivity DNA analysis chips and quantified using Kappa Library
121 Quantification Kit. Paired-end sequencing was performed using 2 x 100bp cycles. The 18 libraries were
122 sequenced on two Illumina Hiseq lanes.

123 Reads quality assessment and filtering

124 Galaxy interface (Giardine et al. 2005) was used to visualize sequencing outputs and filter out low
125 quality reads. Visualization was performed using FastQC. Reads were truncated until the last
126 nucleotide displayed a Phred score of at least 25. Reads shorter than 70 bp or with an average Phred
127 score lower than 25 were removed. Cutadapt was used to remove sequences corresponding to the
128 TruSeq indexed adapter, TruSeq Universal Adapter, dinoflagellate Spliced Leader (Zhang et al. 2007),
129 as well as poly-A tails. For the 18 *A. minutum* strains sequenced, more than 68.10^9 bases were
130 generated of which about 4.10^9 (~ 6%) were discarded after quality filtering.

131 Obtaining *A. minutum* reference transcriptome

132 After initial quality filtering, overlapping paired-end reads were merged using Flash (Magoc and
133 Salzberg 2011). Sequences shorter than 70bp were removed. Merged paired-end reads, as well as non-
134 overlapping paired-end and orphan reads from the 18 strains were used to perform a de novo assembly
135 of *A. minutum* transcriptome using Trinity (Haas et al. 2013) after pooling the reads of the 18 strains.
136 Only transcripts longer than 200bp were retained. A total of 216,203 transcripts were generated
137 representing more than 178.10^6 bases of sequence and an average sequence length of 824 bases. When
138 several isoforms were detected, only the longest one was retained for the analyses, representing
139 153,222 transcripts for a total of 117,601,765 bp with an average transcript size of 767 bp. Sequence
140 similarity of the transcripts with genes of identified function in the UniProt databank was investigated

141 using the bank to bank sequence similarity search tool ngKLAST v4.3 using the KLASTx algorithm
142 (Nguyen and Lavenier 2009) with E-Value $< 10^{-3}$ (32,948 transcripts with homologs). The transcripts
143 were classified in various Gene Ontology categories (GO; <http://geneontology.org/>) based on this
144 result. Independently from this annotation, Transdecoder (Haas et al. 2013) was used to determine
145 Coding Sequences (CDS) from the transcripts (76,698 transcripts with CDS). When more than one
146 possible frame was detected (17,492 CDS, ie ~ 23%), the CDS was not considered unless it contained
147 mutations (see below), in which case the frame minimizing the number of non-synonymous mutations
148 was retained (9,032 CDS). The effect of this choice on the ratio of non-synonymous mutations per
149 transcript is illustrated in supplementary fig. S1 (Supplementary Material online). The analyses were
150 also performed after excluding all the transcripts with more than one possible frame, without any
151 impact on the conclusions (data not shown). As *A. minutum* is not closely related to any model
152 organism, transcript annotation has to be taken with great caution. As a mean to both evaluate at what
153 point annotations maybe meaningful, and decrease the amount of wrongly annotated transcripts the
154 frames assigned by the ngKLAST annotation and the ones inferred from Transdecoder were
155 compared. A total of 26,487 transcripts had frames assigned by both Transdecoder and ngKLAST of
156 which 17,235 did match (65%). This is about 4 times more than expected if the annotation was
157 biologically irrelevant (as there are 6 possible frames random matches are expected for 1/6 of the
158 transcripts). When the two frames did not match, the frame inferred using Transdecoder was
159 conserved, but the annotation was discarded.

160 Alignment to the reference transcriptome

161 The 18 strains were then individually aligned to the reference consisting of 153,222 transcripts with
162 Bowtie2 (Langmead and Salzberg 2012) using paired-end reads. Only reads with a mapping score $>$
163 10 were retained. Alignments were sorted and duplicates removed using Samtools (Li et al. 2009).
164 Taking into account all strains together, sites had an average sequencing depth of 462. Individually,
165 the strains had an average sequencing depth ranging from 11 to 49.

166 Mutation analyses

167 For variant analyses, only transcripts with more than 100 sites covered more than ten times in each of
168 the 18 strains were considered. Single Nucleotide Polymorphisms (SNPs) were detected using

169 FreeBayes (Garrison and Marth 2012). In culture conditions, *A. minutum* cells are in a vegetative,
170 haploid stage. We took advantage of this to remove spurious SNPs and more specifically SNPs that
171 may be identified because of genetic polymorphism within a single genome (in case of paralogy) and
172 not between genomes. To do so, FreeBayes was run with three sets of parameters: 1. haploidy
173 enforced, 2. diploidy enforced and 3. diploidy enforced with a minimal allele count supported by at
174 least 5 reads to call a genotype. Mutations identified by Freebayes were then filtered using VCFtools
175 (Danecek et al. 2011), only keeping positions involved in SNPs, with two alleles, a quality criterion >
176 40, and covered more than 10 times in each of the 18 sequenced strains. Because cultures are
177 composed of haploid clones, diploid enforced genotypes must be homozygote. After filtering, the
178 results of the three Freebayes runs were compared and only positions identified in the haploid
179 enforced run and identified as homozygous in the two diploid enforced runs were considered.
180 Genotypes identified as heterozygotes in the diploidy enforced runs were discarded. Genetic distance
181 among any two strains was calculated as the proportion of variant sites. Hierarchical clustering
182 analysis with complete linkage was performed in R using hclust.

183 To investigate the divergence between group A and B (see Results), the demographic history was
184 analyzed from their joint site frequency spectrum (JSFS) using $\delta\delta i$ v1.7.0 (Gutenkunst et al. 2009).
185 As proposed by Tine et al. (2014), we tested seven alternative models of historical divergence: Strict
186 Isolation (SI), Isolation with Migration (IM), Ancient Migration (AM), Secondary Contact (SC), as
187 well as a version of IM, AM, and SC including a restricted migration rate for a subset of SNPs (IM2m,
188 AM2m, and SC2m). As the ancestral states of the SNPs could not be determined with confidence, we
189 used folded joint frequency spectrum, i.e. the frequency spectrum based on minor allele count. The
190 demographic history was inferred using all polymorphic sites, as well as using five subsets composed
191 of a single randomly chosen synonymous polymorphic site per transcript. For each demographic
192 model and each dataset, more than 30 runs were performed to identify the maximum likelihood and
193 the corresponding parameter estimates. Using this modeling approach, the SNPs observed as fixed
194 (one allele in all members of group A and the alternative allele in all members of group B) were
195 identified as displaying a highly restricted gene flow between the two groups (see Results). We note

196 that when we refer to fixed polymorphism, we considered the observed pattern in the 18 strains
197 studied and do not extrapolate the fixation at the entire group level.

198 Fisher exact tests were used to investigate the deviation from random accumulation of fixed SNPs in
199 the transcripts. False Discovery Rate (FDR) correction for multiple testing with a significance
200 threshold set at $q\text{-value} = 0.05$ was used.

201 Following a McDonald and Kreitman (1991) approach, we used Fisher Exact tests to investigate
202 whether NS mutations are over-represented in the fixed differences.

203 Over-representation of 1. SNPs, 2. Non-Synonymous (NS) SNPs, 3. Fixed SNPs, and 4. Fixed NS
204 SNPs in GO categories was tested for GO categories represented by at least 5 transcripts, using Fisher
205 Exact tests followed by FDR correction for multiple testing with a significance threshold set at $q\text{-value}$
206 $= 0.0001$ (a very stringent FDR was set to balance the uncertainty of the GO annotations due to the
207 absence of a closely related model organism). Only GO categories containing > 5 mutated transcripts
208 were considered. Over-representation analyses were based on SNPs rather than on mutated transcripts
209 to add more weight to the transcripts carrying multiple SNPs.

210 Saxitoxin, COI and rRNA genes

211 Two forms homolog to the cyanobacteria *sxtA* gene, named long and short forms, as well as one
212 homologous of the *sxtG* cyanobacteria gene known to be involved in saxitoxin production were
213 identified in *Alexandrium* (Stüken et al. 2011). We searched the *A. minutum* reference transcriptome
214 generated above for the *A. fundyense sxtA* short (JF343238) and long (JF343239) forms well as *sxtG*
215 (JX995121) using blastn 2.2 (Zhang et al. 2000). Similarly, we searched for published COI
216 (AB374235) and rRNA (AY831408) sequences in the *A. minutum* reference transcriptome generated
217 above using blastn 2.2.

218 Inter-group differential expression

219 Differential expression analyses were performed using the packages, DESeq2 (Love et al. 2014),
220 edgeR (Robinson et al. 2010) and limma (Ritchie et al. 2015) in R. Only transcripts with a total read
221 count higher than 200 were considered, representing 100,797 transcripts with a median coverage per
222 transcript ranging from 42 to 188 reads for the different strains (mean range: 108-505). Hierarchical
223 clustering was performed using hclust (R) based on the Euclidean distance calculated by the dist

224 function (R) on the rlog transformed count matrix. Differential expression between the two groups of
225 strains was tested with a significance FDR threshold set at q-value = 0.05, with rlog (Deseq2), TMM
226 (edgeR), and voom (limma) normalization. The transcripts significant with the three methods
227 (intersection) were considered as differentially expressed. We note that differentially expressed
228 transcripts may be the result of differential regulation of gene expression in the two groups of strains,
229 but also of deletion of the encoding genes in one of the two groups. Over-representation of GO
230 categories was tested for GO categories represented by at least 5 transcripts, using Fisher Exact
231 followed by a False Discovery Rate (FDR) correction for multiple testing with a significance threshold
232 set at q-value = 0.01. Only GO categories containing > 5 differentially expressed transcripts were
233 considered. We note that the presence of a conserved spliced leader in 5' of all dinoflagellate mRNA
234 might indicate important post-transcriptional regulation of gene expression in these organisms (Zhang
235 et al. 2007).

236 Morphological analyses of the strains

237 Thecal plate pattern and the presence of a ventral pore on the first apical plate (1') of the different
238 strains was analyzed after staining thecae with Fluorescent Brightener 28 (Sigma Aldrich) according
239 to the method of Fritz and Triemer (1985). Strains were observed on a slide covered with a coverslip
240 in epifluorescence microscopy after adding a drop of 1% (w/v) of the fluorophore and using a BX41
241 (Olympus, Tokyo) upright microscope fitted with a 100 W mercury lamp and epifluorescence (U-
242 MWU2 filter cube).

243

244 Results

245 Genetic diversity

246 To investigate genetic diversity, we only considered transcripts with more than 100 sites
247 covered more than ten times in each of the 18 sequenced strains, representing a total of 24,630,108
248 sites in 45,089 transcripts, and identified a total of 457,368 polymorphic sites (~1.9 % of the sites) in
249 41,698 transcripts (~92.5% of the transcripts, table 1). We performed a hierarchical clustering analysis
250 based on the nucleotide divergence among any two strains (fig. 1a). Two groups of strains may be
251 distinguished. The first group, hereafter named group A, of 15 strains composed of a slightly divergent

252 strain isolated from Cork (Ireland), and two sub-clades grouping on the one hand all the strains
253 isolated from the Penzé estuary (France) and on the other strains isolated from the Bay of Brest
254 (France) and one strain isolated from the Rance estuary (France). In this group the median number of
255 variable sites among any two strains is 99,224 (~22% of the variable sites), representing a nucleotide
256 divergence of ~0.004, reflecting a high level of genetic diversity (fig. 1a, black). The second group,
257 hereafter named group B, is composed of three strains, one isolated from the Bay of Brest and two
258 from the Bay of Concarneau. Within this group B, the three strains are also very divergent genetically,
259 with a median of 127,407 variable sites among strains (~28%), representing a nucleotide divergence of
260 ~0.005. The intergroup median number of variable sites is 147,913 (~32%), representing a nucleotide
261 divergence of ~0.006. A total of 193,325 variants are singletons, i.e. they were identified in a single
262 strain, representing more than 42% of the identified variants. Looking at the repartition of these
263 singletons in the 18 strains, the two groups of strains previously identified are again clearly visible.
264 Within group A, the median number of singletons is 7,303 (fig. 1b, black). Within group B there is
265 almost 4 times more singletons per strain (median=27,532) (fig. 1b, red).

266

267 Divergence between group A and B

268 To replace the divergence between group A and B in a classical phylogenetic context, we note that in
269 the transcript corresponding to the ribosomal RNA, two SNPs observed as fixed (one allele in all
270 members of group A and the alternative allele in all members of group B) are identified in the 5'
271 external transcribed spacer but none in the region corresponding to the 18S, ITS1, 5.8S, ITS2, and
272 LSU. Similarly, no SNP was identified in the transcript corresponding to the cytochrome c oxidase
273 subunit I (COI), another gene often used to identify closely related species (table 2).

274 To better grasp the patterns of divergence between strains belonging to group A and B and gaining
275 insights on the underlying evolutionary processes, we analyzed the demographic history of groups A
276 and B using their joint site frequency spectrum (JSFS), exploring seven scenario of divergence (fig.2).
277 The simplest model, involving divergence without any gene flow (SI, fig. 2, Supplementary table 1)
278 did not explain the data as well as models involving some amount of gene flow after the split. Of
279 these, the secondary contact (SC) model had the best likelihood, especially because it explained the

280 low occurrence of minor allele only observed in group A (fig. 2). The only part of the JSFS not
281 correctly explained by the SC model was an excess of observed fixed polymorphism compared to the
282 model prediction (lowest residual values, fig. 2). The observed fixed polymorphism was correctly
283 estimated when a heterogeneous migration rate across SNPs, with a fraction of the sites displaying a
284 highly restricted gene flow between groups, was introduced in the divergence model (SC2m model,
285 fig. 2, Supplementary table 1). Similarly, when considering subsets of the entire dataset composed of a
286 single randomly chosen synonymous polymorphic site per transcript, the model with the highest
287 likelihood was the SC2m model (Supplementary table 2). These analyses indicated an ancient
288 divergence of the A and B groups in total isolation, followed by a secondary contact resulting in gene
289 flow between the two groups that is heterogeneous across the genomes, with a fraction of the SNPs
290 displaying highly restricted gene flow. As seen in Figure 2, the polymorphic sites that are observed as
291 fixed between the two groups are the ones displaying restricted gene flow (part of the folded JSFS
292 requiring a heterogeneous migration rate across genomes to be correctly explained, fig. 2).

293 In the dataset, 12,188 variant sites (5% of the variable sites, excluding singletons) display a fixed
294 difference between group A and B (table 1). We focused on the fixed differences between groups A
295 and B to determine if these SNPs are restricted to a few transcripts or randomly distributed in the
296 transcripts. The 12,188 fixed differences occur in 6,215 transcripts but are over-represented, compared
297 to the other differences, in 927 transcripts (Fisher exact test, q-value < 0.05, fig. 3a, red dots),
298 representing 4,616 fixed mutations (38% of the fixed differences). This result clearly points toward a
299 preferential accumulation of the fixed differences in some transcripts.

300 Next, we investigated whether mutations are synonymous (S) or non-synonymous (NS). Excluding
301 singletons, a total of 44,880 NS and 176,609 S mutations were identified in 29,089 transcripts (table
302 1). Focusing on the fixed differences, 3,818 NS and 5,733 S mutations were detected in 4,916
303 transcripts, indicating that non-synonymous mutations are 2.77 times more frequent in the fixed
304 differences compared to the other mutations (Fisher exact test, p-value < $2.2e^{-16}$). More precisely, the
305 frequency of non-synonymous mutations in the transcripts is higher when considering fixed mutations
306 (fig. 3b grey), not only in the transcripts where fixed mutations are over-represented (fig. 3b red), but
307 also in the transcripts only displaying a few fixed mutations (fig 3b blue). This indicates that potential

308 modification of protein functions associated with the divergence is not only linked to transcripts
309 displaying numerous fixed mutations, but also to the transcripts only displaying a few fixed mutations.

310

311 Functional genetic divergence

312 We used two approaches to investigate the functions of the genes displaying fixed differences. In the
313 first one, we analyzed the repartition of SNPs associated to the different gene product properties, as
314 defined by Gene Ontology (GO). A total of 9,508 transcripts representing 82,805 mutations could be
315 associated to GO categories (table 1). We tested whether mutations are over or under represented in
316 the different GO categories. Considering the entire dataset, 24 GO categories display an excess of
317 mutations and 147 display less mutations than expected (fig. 4, 171 GO categories Overall). The non-
318 synonymous mutations were over-represented in 6 categories and underrepresented in 6 (fig. 4, 12 GO
319 categories Overall Non-synonymous). Focusing on the fixed differences, mutations were over-
320 represented in 33 categories (Non-synonymous mutations, 4 categories) and not under-represented in
321 any GO category (fig. 4 Fixed and Fixed Non-synonymous). These fixed differences are found in a
322 total of 328 transcripts. Of special interest are 130 transcripts involved in 5 GO categories related to
323 calcium binding and fluxes across membranes (fig. 4 red) and 44 in 4 GO categories related to
324 potassium fluxes across membranes (fig. 4 blue).

325 In a second approach to grasp the functional bases of the divergence, we focused on the 25 transcripts
326 displaying most fixed genetic divergence between the divergent groups (lowest q-value, fig. 3a, i.e.
327 ~0.5‰ (25/45,089) transcripts displaying the highest level of genetic divergence (table 2). Out of these
328 25 transcripts, 14 were identified as homologs to genes encoding for proteins with known functions.
329 Of extreme interest was the presence of four transcripts homologs to genes involved in calcium
330 mediated transduction signals: two involved in calcium transport (Polycystin-2 and Sodium/calcium
331 exchanger 3), one intermediate messenger transducing calcium signals by binding calcium ions
332 (Calmodulin-like protein 6), and one calcium-dependent protein kinase thought to function in signal
333 transduction pathways that utilize changes in cellular Ca^{2+} concentration to couple cellular responses
334 to extracellular stimuli (Calcium-dependent protein kinase 13). Even more interesting, was the genetic
335 divergence of a transcript corresponding to the short form of the *sxtA* gene, a gene known to be

336 involved in saxitoxin production in cyanobacteria. It contains domains 1 to 3 homologous to the *sxtA*
337 genes found in cyanobacteria and a last translated region that has no homolog in databases except the
338 end of the short *sxtA* form from *A. fundyense* (Stüken et al. 2011). Moreover, these fixed differences
339 include numerous NS mutations (9), two of them being in the first domain (*sxtA1*, corresponding to
340 the amino acids 28-531), one in the second domain (*sxtA2*, amino acids 535-729), none in the third
341 (*sxtA3*, amino acids 750-822) and six in the last translated part of the transcript (amino acids 822-976)
342 (Fig. 2C).

343

344 Differential gene expression

345 We analyzed the mRNA sequences to investigate differential gene expression *in vitro*. First, a
346 clustering analysis based on the expression levels clearly indicates that the two groups of strains
347 identified above using genetic information are also identified using global expression data (fig. 5a).
348 Differential expression was analyzed between group A and group B strains, and a total of 1,518
349 transcripts were identified as differentially expressed (q-value<0.05; fig. 5b; Supplementary Table 3),
350 but no gene ontology category was identified as over or under-represented in the differentially
351 expressed transcripts at a FDR level < 0.1.

352

353 Morphology

354 The 18 strains were stained with Fluorescent Brightener 28 and observed blindly, i.e. without knowing
355 which strains belonged to group A and B in epifluorescence microscopy to analyze the thecal plate
356 pattern. No difference of the thecal organization was found among strains which all possessed the
357 typical plate pattern of *A. minutum*. However, the presence of a ventral pore on the right side of the 1'
358 plate was found on the three strains belonging to group B while the 15 strains belonging to group A
359 lacked this feature (fig. 6).

360

361 Discussion

362

363 Analyzing mRNA sequences in 18 *A. minutum* strains, we identified the divergence of two groups,
364 represented by 15 and 3 strains, respectively. The identification of these two groups was incidental,
365 explaining the unbalanced sampling and illustrating the possibility for reverse ecology approaches to
366 uncover cryptic diversity. This divergence was not detectable using the classical barcoding loci ITS
367 and COI, but the analysis of a transcriptome wide SNPs dataset pointed toward the presence of two
368 distinct evolutionary units. A genetic distance analysis clearly indicated the presence of the two
369 groups. A consistent observation is the difference in the number of singletons identified in the strains
370 belonging to the groups A and B, clearly pointed toward the sampling of two independent genetic
371 entities. Differential expression, although less dramatic than genetic divergence, also goes in the same
372 direction, with the strains belonging to the two groups displaying the most difference in terms of
373 global expression profile. One of the strains was isolated from the natural environment in 1989
374 (Am89) and maintained ever since (i.e. during 24 years, corresponding to ~3,000 generations of
375 cellular division) in batch culture involving bi-weekly transfer in the culture media used in the present
376 work. The other strains were isolated from 2010 to 2013 and maintained in the same culture regime (6
377 months to 3 years of lab culture, 60-350 generations). Despite the difference in the time spent in the
378 laboratory environment and thus experiencing the associated strong selective pressures, the strain
379 Am89 is genetically indistinguishable from the other strains belonging to group A. It illustrated that,
380 compared to the standing genetic variation encountered in natural populations, there are very few
381 mutations that occurred during the long term maintenance in culture. In term of gene expression,
382 Am89 clusters at the base of group A, pointing toward a more extensive evolution of gene expression
383 profile, but still insufficient to overcome the difference in global expression profile occurring between
384 groups A and B.

385 Following the analysis of the mRNA sequences and the identification of the two diverging groups, a
386 morphological difference, the presence/absence of a ventral pore was identified. This morphological
387 character seems diagnostic of the two groups, suggesting the occurrence of two pseudo-cryptic (or
388 pseudo-sibling) species (Knowlton 1993), but caution must be taken due to the very limited sampling
389 of one of the two group. Nonetheless, this morphological character is especially interesting to replace
390 our study in a biogeographical context. Indeed, this morphological feature has been reported in *A.*

391 *minutum* studies with some indication that the morphotype with ventral pore may be more frequent in
392 Southern Europe and the one lacking the ventral pore more frequent in Northern Europe (Hansen et al.
393 2003). Interestingly the two types have also been reported in mixed communities (Western Ireland,
394 Hansen et al. 2003; in the present study Am1072 (group B) and Am1080 (group A) were isolated from
395 the same day and locality) which rules out complete allopatry.

396 Using the SNPs dataset, we investigated the process of divergence between groups A and B. We
397 compared the joint site frequency spectrum of these two groups to the patterns expected following
398 seven models of divergence. The most likely scenario involves an ancient divergence in complete
399 isolation followed by a secondary contact involving gene flow between the two groups. Quite
400 interestingly, the introduction of a heterogeneous migration rate across the genome, with a fraction of
401 the genome displaying a highly restricted gene flow, considerably improved the likelihood of the
402 models. So far only a handful of studies have considered heterogeneous gene flow across the genomes
403 when investigating the divergence of population/species. We note that models of divergence in
404 isolation followed by a secondary contact allowing gene flow between diverging populations/species,
405 but at different rates across the genome, are, so far, almost always the best at explaining the observed
406 allelic frequencies in ascidian (Roux et al. 2013), mussels (Roux et al. 2014), fishes (Tine et al. 2014,
407 Le Moan et al. 2016, Rougemont et al. 2016), and Ascomycota (Gladieux et al. 2015). Here, an
408 extremely low migration rate at a fraction of the genome is required to explain the observed pattern of
409 fixed polymorphism, i.e. of polymorphism with all members of group A displaying one allele, and all
410 members of group B displaying the alternative allele. This fixed polymorphism corresponds to about
411 5% of the SNPs displaying a heterogeneous distribution in the various transcripts. This is similar to the
412 pattern reported in studies investigating recent or ongoing speciation events at the genome scale
413 (Seehausen et al. 2014). However, one of the caveat of using transcriptome and not genome wide data
414 is that the information regarding the physical linkage between the genes encoding for the transcripts is
415 lacking. As a result, we do not know whether the transcripts displaying high levels of genetic
416 divergence are physically linked in a few genomic islands of divergence (Turner et al. 2005) or if they
417 are spread out in the genome.

418 We compared the proportion of non-synonymous polymorphism segregating and fixed between the
419 two groups and identified a strong excess of non-synonymous polymorphism in the fixed mutations.
420 SNPs fixation within each group, but divergence between groups associated with overrepresentation of
421 NS SNPs is difficult to explain with demographic fluctuations or relaxed selection and points toward
422 the importance of selection as a driving force of the divergence between the two groups. This pattern
423 could reflect classic selective sweeps, i.e. the fixation of adaptive mutations in either group, and the
424 associated hitchhiking of physically linked neutral mutations (Nielsen 2005). Interestingly, an excess
425 of fixed non-synonymous mutations was also identified in transcripts only displaying a few fixed
426 polymorphic sites, often associated with segregating polymorphism. This excess of NS mutations
427 suggests that mutations associated with the functional divergence of the two divergent groups are not
428 systematically associated with a selective sweep, i.e. may get to fixation without a drastic reduction of
429 diversity at neighboring sites. Indeed the pattern of linkage disequilibrium associated to an adaptive
430 mutation is influenced by numerous factors including, the strength of selection, local levels of
431 recombination, and whether adaptive mutations are *de novo* mutations or were segregating in ancestral
432 populations before becoming adaptive (Fay and Wu 2000; Przeworski et al. 2005; Lee et al. 2014).

433 The selective pressures responsible for restricted and heterogeneous gene flow may be directly linked
434 to the ecological divergence of the two groups. It could for example be the case, if the two groups
435 occupy geographically and ecologically distinct habitats and only encounter each other and exchange
436 genes at localized hybrid zones. In this case, introgression of neutral SNPs from one group to the other
437 would occur more or less freely, while the introgression of the SNPs responsible for local adaptation
438 of each group would be counter selected. An alternative scenario could involve the build-up of
439 reproductive isolation between the two groups. For example, gene flow could be restricted overall if
440 members of the two groups are not likely to recognize each other as proper mates, and negative
441 epistasis between sets of SNPs could lead to reduced hybrid fitness depending (hybrid maladaptation)
442 or not (genetic incompatibilities) on the environmental conditions. Distinguishing between these
443 different scenarios (none of them being mutually exclusive) would require extensive sampling from
444 the natural environment, crossing experiments and fitness assays that are beyond the scope of the

445 present work. However, investigating the cellular functions of the transcripts displaying restricted gene
446 flow between the two groups could help pointing in one direction.

447 Transcripts related to potassium and calcium fluxes across membranes were identified as carrying
448 more fixed polymorphism than expected. Moreover, among the transcripts displaying the highest
449 levels of divergence, four could be related to calcium mediated transduction signals, and one was
450 homologous to *sxtA*, a gene involved in saxitoxin production (Stüken et al. 2011). Two genetically
451 divergent forms of *sxtA* have been identified in *Alexandrium* transcriptomes (Stüken et al. 2011). Here,
452 the *sxtA* identified as highly divergent between the two groups corresponds to the short form, which is
453 probably not involved in saxitoxin production (Murray et al. 2015; the long form was also identified in
454 all strains, but without displaying a pattern of divergence, data not shown). As a result, we hypothesize
455 that the molecule of interest associated with the divergence of the two groups might not be the
456 saxitoxin itself but another compound synthesized via the saxitoxin biosynthesis pathway. There may
457 be a direct link between *sxtA*, genes related to calcium and potassium fluxes, and calcium mediated
458 signal transduction. Indeed, although the saxitoxin toxicity occurs through the blocking of mammal
459 sodium channels, it is also known to bind to mammal calcium and potassium channels, modifying
460 calcium and potassium fluxes without entirely blocking them (Cusick and Sayler 2013). This analysis
461 points toward a molecular mechanism that may be at play during the divergence of the two groups, but
462 does not indicate whether it is related to ecological divergence or the build-up of reproductive
463 isolation. In favor of the build-up of reproductive isolation, saxitoxin has been proposed to act as a sex
464 pheromone in natural environment (Wyatt and Jenkinson 1997; Cusick and Sayler 2013) and another
465 guanidine alkaloids marine toxin, the tetrodotoxin, has been shown to act as sex pheromone
466 (Matsumura 1995). However, some *Alexandrium* strains do not produce the toxin and would thus be
467 unable to attract proper mates, but as discussed above, the molecule at play here is probably not the
468 saxitoxin itself but a related molecule. In favor of an ecological divergence, we may cite the proposed
469 role of saxitoxin as a grazer deterrent (Cusick and Sayler 2013), but it would require a specialized
470 relationship to exert a selective pressure responsible for the observed divergence. Finally, unicellular
471 motility is often linked to calcium fluxes across the membrane (Verret et al. 2010), with potential
472 implications in both ecological divergence and reproductive isolation.

473

474 To conclude, using a reverse ecology approach based on the mRNA sequencing and morphology
475 analysis of several strains of the dinoflagellate *A. minutum*, two diverging groups, co-occurring in
476 nature, were identified. The most likely scenario of divergence involved ancient divergence in
477 complete isolation followed by a secondary contact resulting in gene flow, heterogeneous across the
478 genome, between the diverging groups. The SNPs subjected to restricted gene flow also display an
479 overrepresentation of fixed non-synonymous polymorphism. This highlights the importance of the
480 functional aspect of the divergence, and identifies selection as a potential major evolutionary force
481 driving this event. At the molecular level the functions associated with the divergence are especially
482 related to toxin production and calcium/potassium fluxes with potential implications in terms of
483 ecological divergence and build-up of reproductive isolation that remain to be tested.

484

485 Acknowledgments: This work was supported by a financial support from the Région Bretagne and the
486 ANR Hapar (ANR-14-CE02-0007-01). We acknowledge RIC and Abims facilities for bioinformatics
487 support, the laboratories LSEM and PFOM for providing access to some of their equipment, Elisabeth
488 Nézan, and Pierre-Alexandre Gagnaire for discussion, four anonymous reviewers, Tatiana Giraud, and
489 Myriam Valero for comments on the manuscript.

490

491 References

492

- 493 Anderson DM, Alpermann TJ, Cembella AD, *et al.* (2012a) The globally distributed genus
494 *Alexandrium*: Multifaceted roles in marine ecosystems and impacts on human health. *Harmful*
495 *Algae* **14**, 10-35.
- 496 Anderson DM, Cembella AD, Hallegraeff GM (2012b) Progress in understanding harmful algal
497 blooms: Paradigm shifts and new technologies for research, monitoring, and management. In:
498 *Annual Review of Marine Science* **4**, 143-176.
- 499 Bierne N, Bonhomme F, David P (2003) Habitat preference and the marine-speciation paradox.
500 *Proceedings of the Royal Society B-Biological Sciences* **270**, 1399-1406.
- 501 Casabianca S, Penna A, Pecchioli E, Jordi A, Basterretxea G and Vernesi C (2011) Population genetic
502 structure and connectivity of the harmful dinoflagellate *Alexandrium minutum* in the
503 Mediterranean Sea. *Proceedings of the Royal Society B-Biological Sciences* **279**, 129-138.
- 504 Casteleyn G, Leliaert F, Backeljau T, *et al.* (2010) Limits to gene flow in a cosmopolitan marine
505 planktonic diatom. *Proceedings of the National Academy of Sciences of the United States of*
506 *America* **107**, 12952-12957.
- 507 Cusick KD, Saylor GS (2013) An overview on the marine neurotoxin, saxitoxin: genetics, molecular
508 targets, methods of detection and ecological functions. *Marine Drugs* **11**, 991-1018.

509 Danecek P, Auton A, Abecasis G, *et al.* (2011) The variant call format and VCFtools. *Bioinformatics*
510 **27**, 2156-2158.

511 Dia A, Guillou L, Mauger S, *et al.* (2014) Spatiotemporal changes in the genetic diversity of harmful
512 algal blooms caused by the toxic dinoflagellate *Alexandrium minutum*. *Molecular Ecology* **23**,
513 549-560.

514 Ellegren H (2014) Genome sequencing and population genomics in non-model organisms. *Trends in*
515 *Ecology & Evolution* **29**, 51-63.

516 Fay JC, Wu CI (2000) Hitchhiking under positive Darwinian selection. *Genetics* **155**, 1405-1413.

517 Feder JL, Flaxman SM, Egan SP, Comeault AA, Nosil P (2013) Geographic mode of speciation and
518 genomic divergence. *Annual Review of Ecology, Evolution, and Systematics, Vol 44* **44**, 73-97.

519 Fritz L, Triemer RE (1985) A rapid simple technique utilizing Calcofluor White M2R for the
520 visualization of dinoflagellate thecal plates. *Journal of Phycology* **21**, 662-664.

521 Garrison E, Marth G (2012) Haplotype-based variant detection from short-read sequencing. Preprint
522 arXiv:1207.3907

523 Giardine B, Riemer C, Hardison RC, *et al.* (2005) Galaxy: A platform for interactive large-scale
524 genome analysis. *Genome Research* **15**, 1451-1455.

525 Gladieux P, Wilson BA, Perraudeau F, *et al.* (2015) Genomic sequencing reveals historical,
526 demographic and selective factors associated with the diversification of the fire-associated
527 fungus *Neurospora discreta*. *Molecular Ecology* **24**, 5657–5675.

528 Gutenkunst RN, Hernandez RD, Williamson SH, and Bustamante CD (2009) Inferring the joint
529 demographic history of multiple populations from multidimensional SNP data. *PLoS Genetics*
530 **5**, e1000695.

531 Haas BJ, Papanicolaou A, Yassour M, *et al.* (2013) De novo transcript sequence reconstruction from
532 RNA-seq using the Trinity platform for reference generation and analysis. *Nature Protocols* **8**,
533 1494-1512.

534 Hansen G, Daugbjerg N, Franco JM (2003) Morphology, toxin composition and LSU rDNA
535 phylogeny of *Alexandrium minutum* (Dinophyceae) from Denmark, with some morphological
536 observations on other European strains. *Harmful Algae* **2**, 317-335.

537 Hutchinson G (1961) The paradox of the plankton. *The American Naturalist* **95**, 137-145.

538 Iglesias-Rodríguez MD, Schofield OM, Batley J, Medlin LK, and Hayes PK (2006) Intraspecific
539 genetic diversity in the marine coccolithophore *Emiliana huxleyi* (Primmnesiophyceae) : The
540 use of microsatellite analysis in marine phytoplankton population studies. *Journal of*
541 *Phycology* **42**, 526-536.

542 Knowlton N (1993) Sibling Species in the Sea. *Annual Review of Ecology and Systematics* **24**, 189-
543 216.

544 Le Moan A, Gagnaire P-A, Bonhomme F (2016) Parallel genetic divergence among coastal–marine
545 ecotype pairs of European anchovy explained by differential introgression after secondary
546 contact. *Molecular Ecology*. doi: 10.1111/mec.13627.

547 Langmead B, Salzberg SL (2012) Fast gapped-read alignment with Bowtie 2. *Nature Methods* **9**, 357-
548 359.

549 Lee YCG, Langley CH, Begun DJ (2014) Differential strengths of positive selection revealed by
550 hitchhiking effects at small physical scales in *Drosophila melanogaster*. *Molecular Biology*
551 *and Evolution* **31**, 804-816.

552 Li H, Handsaker B, Wysoker A, *et al.* (2009) The sequence alignment/map format and SAMtools.
553 *Bioinformatics* **25**, 2078-2079.

554 Li YF, Costello JC, Holloway AK, Hahn MW (2008) "Reverse ecology" and the power of population
555 genomics. *Evolution* **62**, 2984-2994.

556 Love MI, Huber W, Anders S (2014) Moderated estimation of fold change and dispersion for RNA-
557 seq data with DESeq2. *Genome Biology* **15**.

558 Magoc T, Salzberg SL (2011) FLASH: fast length adjustment of short reads to improve genome
559 assemblies. *Bioinformatics* **27**, 2957-2963.

560 Masseret E, Grzebyk D, Nagai S *et al.* (2009) Unexpected genetic diversity among and within
561 populations of the toxic dinoflagellate *Alexandrium catenella* as revealed by nuclear
562 microsatellite markers. *Applied and Environmental Microbiology* **75**, 2037-2045.

563 Matsumura K (1995) Tetrodotoxin as a pheromone. *Nature* **378**, 563-564.

564 McDonald JH, Kreitman M (1991) Adaptive protein evolution at the *adh* locus in *Drosophila*. *Nature*
565 **351**, 652-654.

566 Murray SA, Diwan R, Orr RJS, Kohli GS, John U (2015) Gene duplication, loss and selection in the
567 evolution of saxitoxin biosynthesis in alveolates. *Molecular Phylogenetics and Evolution* **92**,
568 165-180.

569 Nguyen VH, Lavenier D (2009) PLAST: parallel local alignment search tool for database comparison.
570 *Bmc Bioinformatics* **10**.

571 Nielsen R (2005) Molecular signatures of natural selection. *Annual Review of Genetics* **39**, 197-218.

572 Palenik B, Grimwood J, Aerts A, *et al.* (2007) The tiny eukaryote *Ostreococcus* provides genomic
573 insights into the paradox of plankton speciation. *Proceedings of the National Academy of*
574 *Sciences of the United States of America* **104**, 7705-7710.

575 Palumbi SR (1992) Marine speciation on a small planet. *Trends in Ecology & Evolution* **7**, 114-118.

576 Peers G, Price NM (2006) Copper-containing plastocyanin used for electron transport by an oceanic
577 diatom. *Nature* **441**, 341-344.

578 Przeworski M, Coop G, Wall JD (2005) The signature of positive selection on standing genetic
579 variation. *Evolution* **59**, 2312-2323.

580 Ritchie ME, Phipson B, Wu D, Hu Y, Law CW, Shy W, and Smyth GK (2015) limma powers
581 differential expression analyses for RNA-sequencing and microarray studies. *Nucleic Acids*
582 *Research* **43**, e47.

583 Robinson MD, McCarthy DJ and Smyth GK (2010) edgeR: a Bioconductor package for differential
584 expression analysis of digital gene expression data. *Bioinformatics* **26**, 139-140.

585 Rocap G, Larimer FW, Lamerdin J, *et al.* (2003) Genome divergence in two *Prochlorococcus*
586 ecotypes reflects oceanic niche differentiation. *Nature* **424**, 1042-1047.

587 Rougemont Q, Gaigher A, Lasne E, Côte J, Coke M, Besnard A-L, Launey S and Evanno G (2015)
588 Low reproductive isolation and highly variable levels of gene flow reveal limited progress
589 towards speciation between European river and brook lampreys. *Molecular Ecology* **28**, 2249-
590 2263.

591 Roux C, Tsagkogeorga G, Bierne N, and Galtier N (2013) Crossing the species barrier: genomic
592 hotspots of introgression between two highly divergent *Ciona intestinalis* species. *Molecular*
593 *Biology and Evolution* **30**, 1574-1587.

594 Roux C, Fraïsse C, Castric V, Vekemans X, Pogson GH and Bierne N (2014) Can we continue to
595 neglect genomic variation in introgression rates when inferring the history of speciation? A
596 case study in a *Mytilus* hybrid zone. *Journal of Evolutionary Biology* **27**, 1662-1675.

597 Roy S, Chattopadhyay J (2007) Towards a resolution of 'the paradox of the plankton': A brief
598 overview of the proposed mechanisms. *Ecological Complexity* **4**, 26-33.

599 Rynearson TA, and Armbrust VE (2004) Genetic differentiation among populations of the planktonic
600 marine diatom *Ditylum brightwellii* (Bacillariophyceae). *Journal of Phycology* **40**, 34-43.

601 Seehausen O, Butlin RK, Keller I, *et al.* (2014) Genomics and the origin of species. *Nature Reviews*
602 *Genetics* **15**, 176-192.

603 Shores N, Hegreness M, Kishony R (2008) Evolution exacerbates the paradox of the plankton.
604 *Proceedings of the National Academy of Sciences of the United States of America* **105**, 12365-
605 12369.

606 Stomp M, Huisman J, de Jongh F, *et al.* (2004) Adaptive divergence in pigment composition promotes
607 phytoplankton biodiversity. *Nature* **432**, 104-107.

608 Stüken A, Orr RJS, Kellmann R, *et al.* (2011) Discovery of nuclear-encoded genes for the neurotoxin
609 saxitoxin in dinoflagellates. *Plos One* **6**, 12.

610 Tine M, Kuhl H, Gagnaire P-A, *et al.* (2014) European sea bass genome and its variation provide
611 insights into adaptation to euryhalinity and speciation. *Nature Communications* **5**, 5770.

612 Turner TL, Hahn MW, Nuzhdin SV (2005) Genomic islands of speciation in *Anopheles gambiae*. *Plos*
613 *Biology* **3**, 1572-1578.

614 Verret F, Wheeler G, Taylor AR, Farnham G, Brownlee C (2010) Calcium channels in photosynthetic
615 eukaryotes: implications for evolution of calcium-based signalling. *New Phytologist* **187**, 23-
616 43.

617 Weiner A, Aurahs R, Kurasawa A, Kitazato H, Kucera M (2012) Vertical niche partitioning between
618 cryptic sibling species of a cosmopolitan marine planktonic protist. *Molecular Ecology* **21**,
619 4063-4073.
620 Wisecaver JH, Hackett JD (2011) Dinoflagellate genome evolution. *Annual Review of Microbiology*
621 **65**, 369-387.
622 Wyatt T, Jenkinson IR (1997) Notes on *Alexandrium* population dynamics. *Journal of Plankton*
623 *Research* **19**, 551-575.
624 Zhang H, Hou Y, Miranda L, *et al.* (2007) Spliced leader RNA trans-splicing in dinoflagellates.
625 *Proceedings of the National Academy of Sciences of the United States of America* **104**, 4618-
626 4623.
627 Zhang Z, Schwartz S, Wagner L, Miller W (2000) A greedy algorithm for aligning DNA sequences.
628 *Journal of Computational Biology* **7**, 203-214.
629
630
631

632 Data Accessibility:

633 Raw reads and Reference transcriptome: European Nucleotide Archive
634 <http://www.ebi.ac.uk/ena/data/view/PRJEB15046>

635
636 SNP and differential expression information: SEANOE database <http://doi.org/10.17882/45445>
637
638
639

640 Author Contributions:

641 MLG, CD and LG designed research, MLG, GM, NC, PM, JQ and OB performed research, MLG and
642 NC analyzed the data, MLG, GM, NC, RS, CD, LG and AC wrote the paper.
643
644
645

646 Figure legends

647
648 Fig. 1. Genetic divergence. (a) Hierarchical clustering analysis displaying the genetic distance among
649 *A. minutum* strains based on nucleotide divergence, names of the strains and year of isolation are
650 indicated; (b) number of singletons per strain; (c) origin of the strains. The strains from group A are in
651 black and the ones from group B in red.
652

653 Fig. 2. Results of model fitting for seven alternative models of divergence. The observed folded Allele
654 Frequency Spectrum (AFS), as well as for each model, the residuals of the modeled AFS are
655 presented. SI is the strict isolation model. IM is the Isolation-with-Migration model, AM the Ancient
656 Migration model, and SC is the Secondary Contact model. All three models of divergence-with-gene-
657 flow were implemented using one, shared migration rate in each direction ($m_1 > 2$, $m_2 > 1$) across the
658 genome (homogeneous migration), or with two categories of migration rates in each direction across
659 the genome (heterogeneous migration). The data are best explained by the SC2m model.
660

661 Fig. 3. Fixed polymorphism. (a) Repartition of the transcripts based on the number sites displaying
662 fixed and segregating polymorphism. Red dots indicate over-representation of fixed polymorphism (q -
663 value < 0.05). For the 25 most divergent transcripts, homology with genes involved in calcium
664 transduction signal (red) and saxitoxin production (violet) are indicated. (b) Frequency of NS
665 polymorphism considering segregating polymorphism (grey), fixed polymorphism in transcripts where
666 fixed polymorphism is over-represented (red), and fixed polymorphism in transcripts without over-
667 representation of fixed polymorphism (blue). (c) Fixed amino acid substitutions in SxtA.
668

669 Fig. 4. Venn diagram indicating the number of Gene Ontology (GO) categories displaying deviation
670 from random accumulation of mutations (q -value < 0.0001), considering all mutations (Overall), the
671 NS mutations (Overall Non-Synonymous), the fixed mutations (Fixed), and the NS fixed mutations

672 (Non-Synonymous Fixed). For the analyses focusing on the fixed mutations, the name of the GO
 673 categories is given, as well as the number of transcripts mutated, number of mutations, and q-values.
 674 Black arrows indicate over-representation of fixed mutations and white arrows indicate under-
 675 representation of mutations overall.

676
 677 Fig. 5. Gene expression. (a) Hierarchical clustering based on the expression Euclidean distance (rlog).
 678 The strains from group A are in black and the ones from group B in red. (b) MA plot showing for each
 679 transcript the fold change (groupB/groupA) as a function of the average expression. Transcripts
 680 identified as differentially expressed are in red (q-value < 0.05).

681
 682 Fig 6. Epifluorescence micrographs of the 18 strains showing the presence (red arrow) or the absence
 683 (blue arrow) of a ventral pore on the first apical plate of the theca. Scale bars: 20 μ m.

684
 685
 686 Table 1: Summary of transcripts and mutations analyzed, considering the entire dataset (Total), the
 687 transcripts displaying mutations (Mutated), the transcripts displaying mutations excluding singletons
 688 (Mutated no singleton), and the transcript displaying fixed mutations (Fixed).

	Number of Transcripts	Length	Transcripts with CDS	Length CDS (NS)	Transcripts with homolog	Length Annotated (NS)
Total	45,089	24,630,108 ^a	32,797	20,396,618 ^a	10,454	7,703,971 ^a
Mutated	41,698	457,368 ^b	31,111	376,242 ^b (85,923 ^b)	10,029	139,286 ^b (26,725 ^b)
Mutated no singleton	38,116	264,573 ^b	29,089	221,489 ^b (44,880 ^b)	9,508	82,805 ^b (14,007 ^b)
Fixed	6,215	12,188 ^b	4,916	9,551 ^b (3,818 ^b)	1,670	3,408 ^b (1,183 ^b)

689 ^aLength of the transcripts

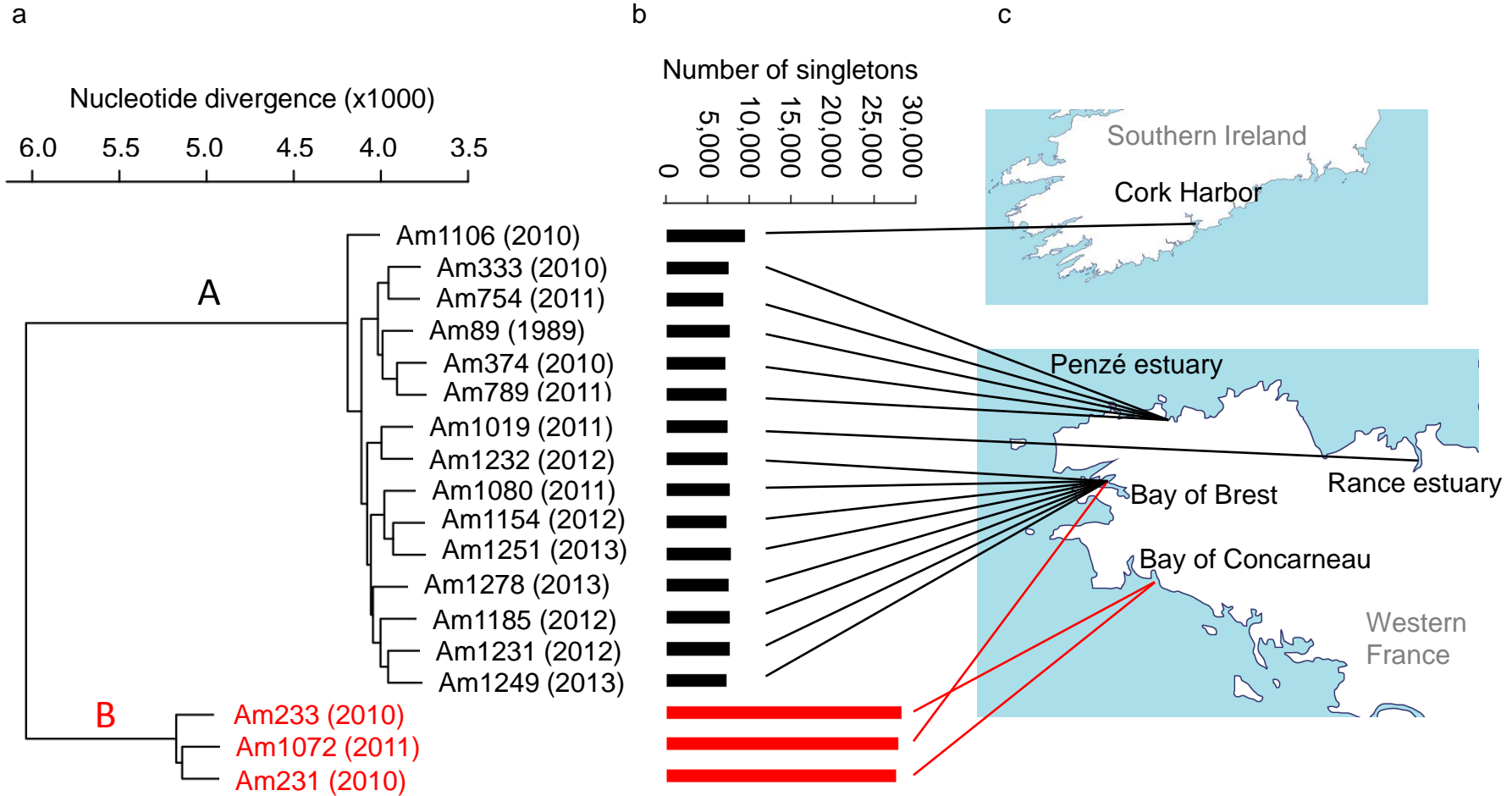
690 ^bNumber of mutations

691
 692
 693
 694
 695
 696
 697
 698
 699
 700
 701
 702
 703
 704
 705
 706
 707
 708
 709

Table 2: Most divergent transcripts between A and B, and loci classically used in phylogenetic studies.

	Name	Fixed Mutations	Not Fixed Mutations	Homologs	E-value	Identity	
25 most divergent transcripts between A and B	comp60373_c0_seq1	22	2	CALL6_HUMAN	Calmodulin-like protein 6	1.10⁻¹⁰	38.1%
	comp98959_c0_seq1	18	0	TGS1_HUMAN	Trimethylguanosine synthase	3.10 ⁻⁴¹	39.1%
	comp102434_c0_seq1	18	3	PKD2_MOUSE	Polycystin-2	2.10⁻¹⁹	35.4%
	comp124736_c0_seq1	15	0	NA			
	comp95518_c0_seq1	16	2	NAC3_HUMAN	Sodium/calcium exchanger 3	2.10⁻¹²⁰	33.3%
	comp86525_c0_seq1	13	0	NA			
	comp101280_c0_seq1	15	4	NA			
	comp101305_c0_seq1	13	1	NA			
	comp75832_c0_seq1	13	2	CMBL_RAT	Carboxymethylenebutenolidase homolog	6.10 ⁻¹²	22.8%
	comp96757_c0_seq1	13	2	NA			
	comp96807_c0_seq1	12	1	NEK5_HUMAN	Serine/threonine-protein kinase Nek5	5.10 ⁻⁰⁵	26.5%
	comp124661_c0_seq5	14	5	PGMC2_ARATH	Glucose phosphomutase 2	1.10 ⁻¹⁶⁴	48.9%
	comp78930_c0_seq1	11	0	NA			
	comp94714_c0_seq1	15	8	NA			
	comp104352_c0_seq1	12	2	NAAA_MOUSE	N-acylethanolamine-hydrolyzing acid amidase	8.10 ⁻³³	29.9%
	comp82584_c0_seq1	11	1	NA			
	comp115853_c0_seq1	13	5	PAMO_THEFY	Phenylacetone monooxygenase	5.10 ⁻⁰⁵	34%
	comp95265_c0_seq1	12	3	NA			
	comp105111_c2_seq1	10	0	EF1A_CRYPV	Elongation factor 1-alpha	3.10 ⁻⁹⁶	46.2%
	comp106635_c0_seq1	10	0	CDPKD_ARATH	Calcium-dependent protein kinase 13	1.10⁻³¹	24.9%
comp119140_c0_seq2	10	0	WIPF1_MOUSE	WAS/WASL-interacting protein family member 1	2.10 ⁻⁰⁵	34.3%	
comp86654_c0_seq1	11	2	NA				
comp121041_c0_seq1	15	13	F5BWX9_ALEFU	SxtA short isoform precursor	0.0	63%	
comp117520_c0_seq1	14	14	MSL7_MYCMM	Beta-ketoacyl-acyl-carrier-protein synthase I	7.10 ⁻²²	30.4%	
comp66739_c0_seq1	10	1	ATAD3_BOVIN	ATPase family AAA domain-containing protein 3	7.10 ⁻⁹¹	40%	
COI	comp126209_c0_seq1	0	0	AB374235	A. catenella cox1	0.0	99%
rRNA	comp93300_c0_seq1	2 (ETS)	0	AY831408	A. minutum CCMP113 ETS-18S-ITS1-5.8S-ITS2-LSU	0.0	99%

Upper part, transcripts displaying the highest level of divergence between group A and B (klastx against UniProt/Swissprot). Transcripts with homologs involved in saxitoxin production and calcium signal transduction are indicated in violet, and red, respectively. Lower part, loci classically used in phylogenetic studies (blastn).



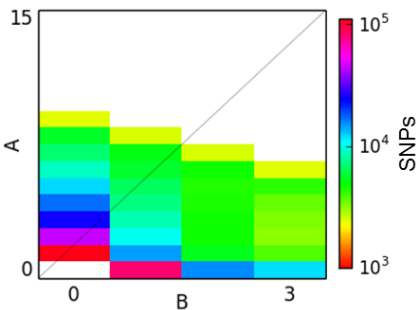
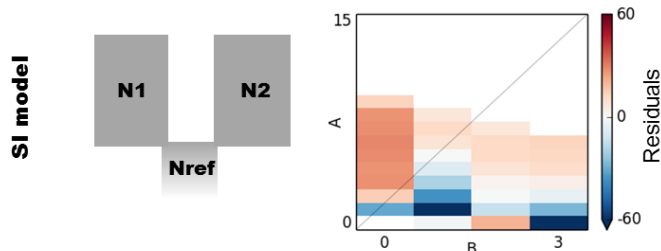
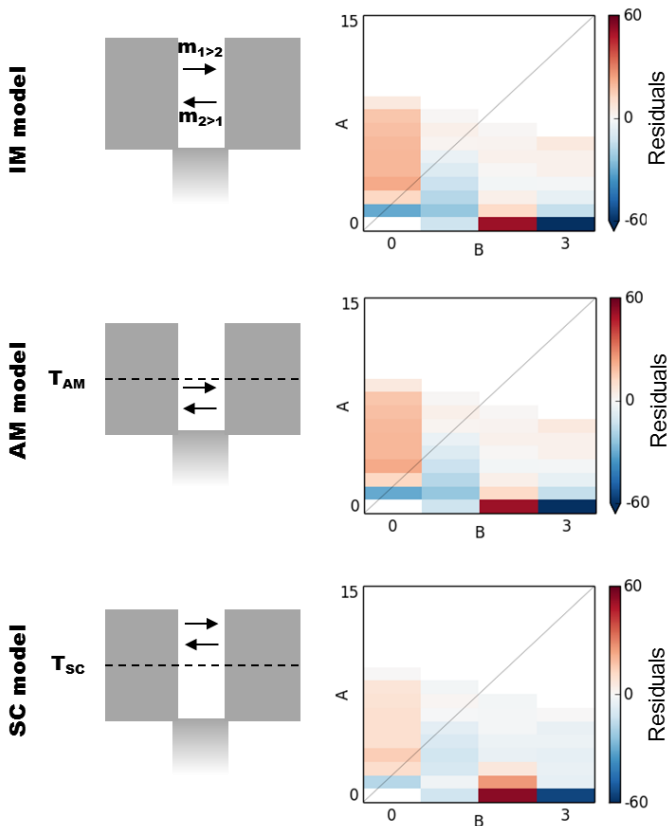
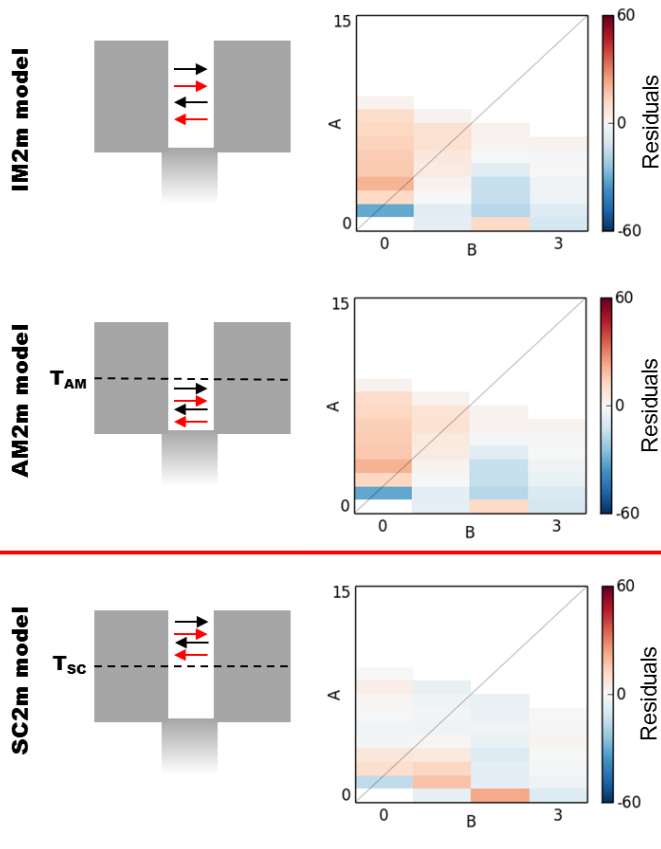
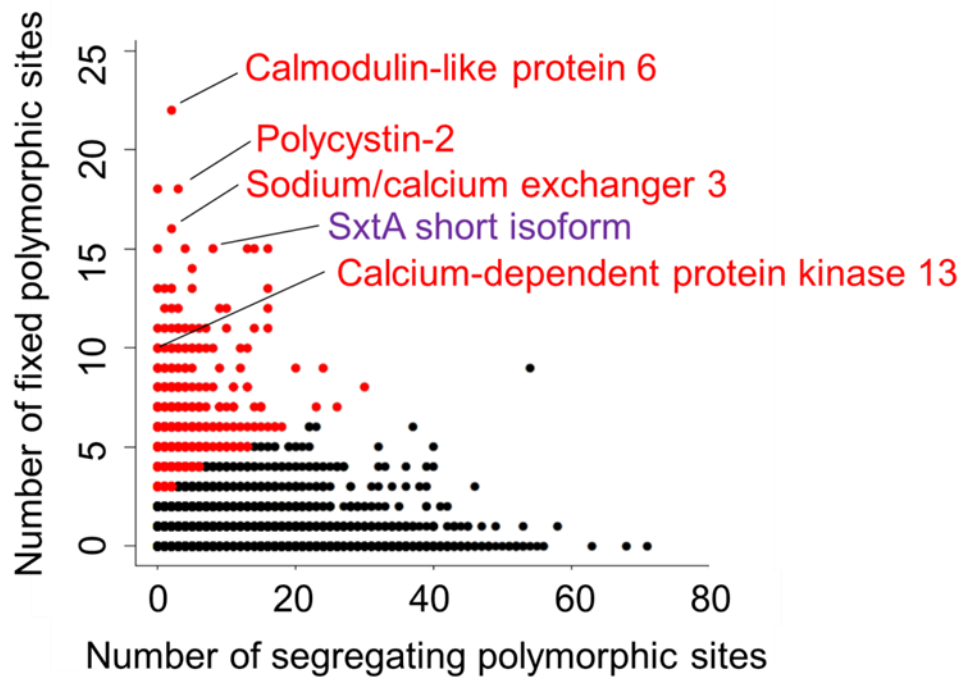
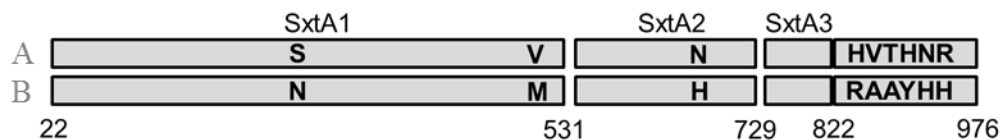
Observed - Folded AFS**Model - No migration****Model - Homogeneous migration****Model - Heterogeneous migration**

Figure 2: Results of model fitting for seven alternative models of divergence. The observed folded Allele Frequency Spectrum (AFS), as well as for each model, the residuals of the modeled AFS are presented. SI is the strict isolation model. IM is the Isolation-with-Migration model, AM the Ancient Migration model, and SC is the Secondary Contact model. All three models of divergence-with-gene-flow were implemented using one, shared migration rate in each direction ($m_{1>2}$, $m_{2>1}$) across the genome (homogeneous migration), or with two categories of migration rates in each direction across the genome (heterogeneous migration). The data are best explained by the SC2m model,

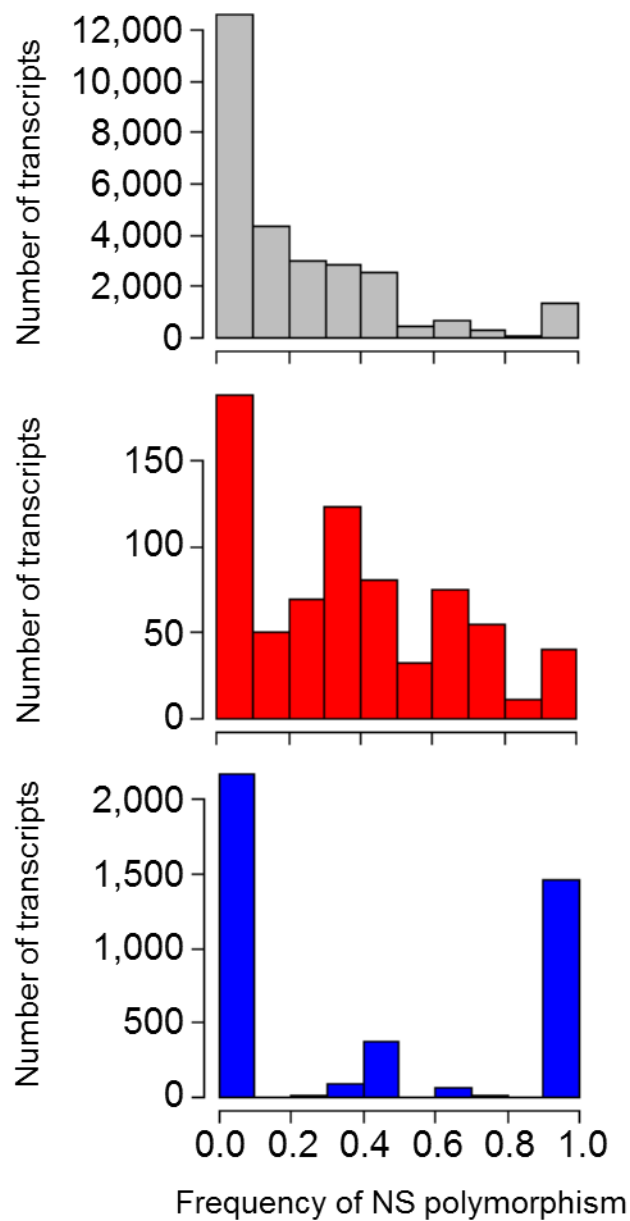
a



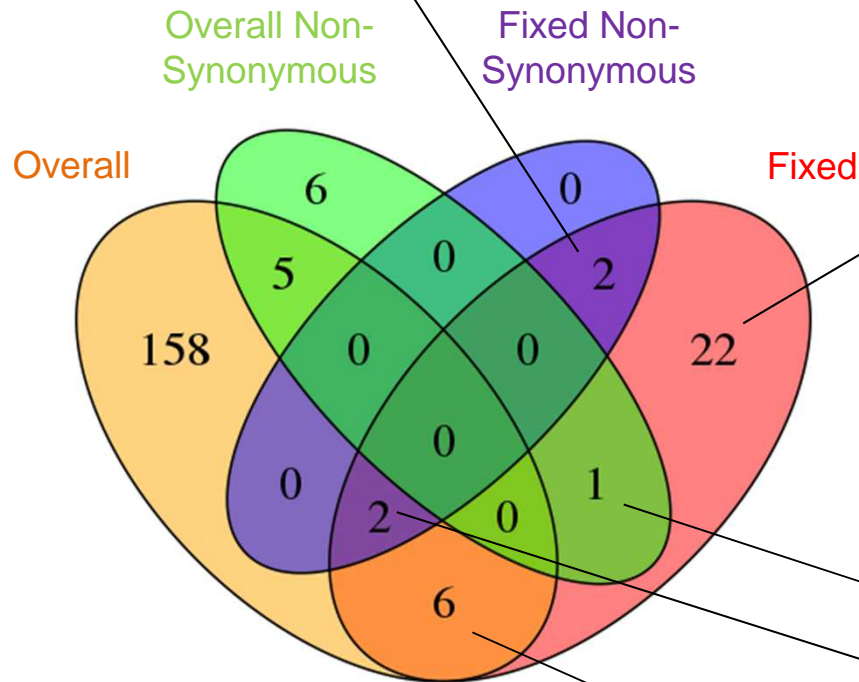
c



b



GO:0005887:integral component of plasma membrane, 35, 115, 2e-14 ↑
 GO:0005249:voltage-gated potassium channel activity, 29, 66, 7e-08 ↑



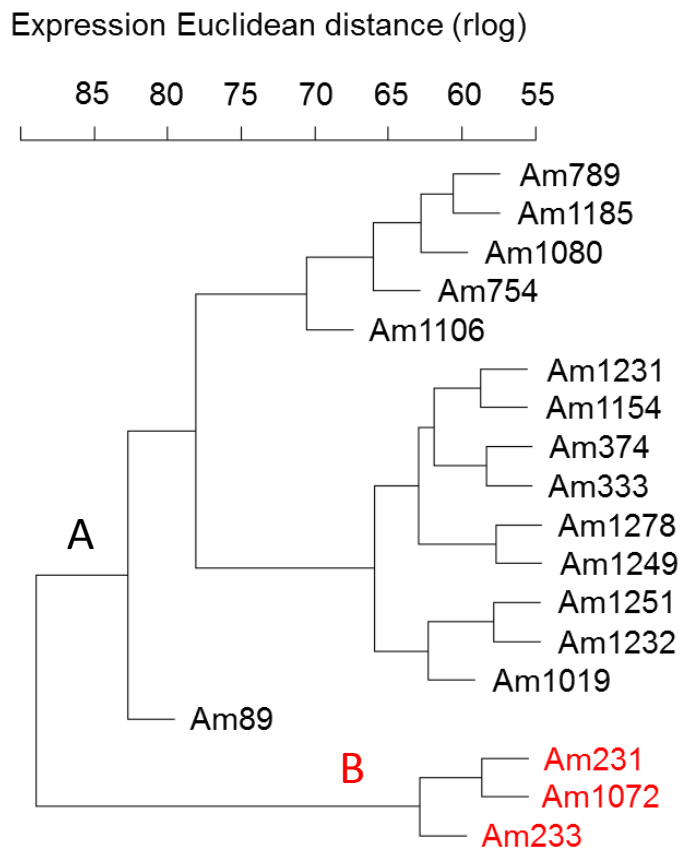
GO:0005432:calcium:sodium antiporter activity, 6, 27, 3e-16 ↑
 GO:0007154:cell communication, 6, 27, 7e-13 ↑
GO:0005245:voltage-gated calcium channel activity, 22, 66, 6e-10 ↑
GO:0006816:calcium ion transport, 18, 63, 1e-09 ↑
 GO:0042597:periplasmic space, 6, 26, 8e-09 ↑
GO:0005262:calcium channel activity, 8, 39, 2e-08 ↑
 GO:0055037:recycling endosome, 7, 22, 3e-08 ↑
 GO:0007596:blood coagulation, 23, 53, 3e-07 ↑
 GO:0050982:detection of mechanical stimulus, 7, 29, 9e-07 ↑
 GO:0051117:ATPase binding, 9, 34, 1e-06 ↑
 GO:0031513:nonmotile primary cilium, 7, 28, 7e-06 ↑
 GO:0071910:determination of liver left/right asymmetry, 6, 28, 7e-06 ↑
 GO:0042391:regulation of membrane potential, 21, 51, 1e-05 ↑
 GO:0005102:receptor binding, 9, 38, 2e-05 ↑
 GO:0045180:basal cortex, 7, 28, 2e-05 ↑
 GO:0015299:solute:proton antiporter activity, 6, 21, 2e-05 ↑
 GO:0009925:basal plasma membrane, 6, 27, 2e-05 ↑
 GO:0007165:signal transduction, 38, 99, 4e-05 ↑
GO:0005267:potassium channel activity, 8, 27, 6e-05 ↑
 GO:0072686:mitotic spindle, 8, 29, 7e-05 ↑
GO:0005509:calcium ion binding, 100, 272, 8e-05 ↑
 GO:0016998:cell wall macromolecule catabolic process, 7, 16, 1e-04 ↑

GO:0019897:extrinsic component of plasma membrane, 6, 20, 1e-06 ↑

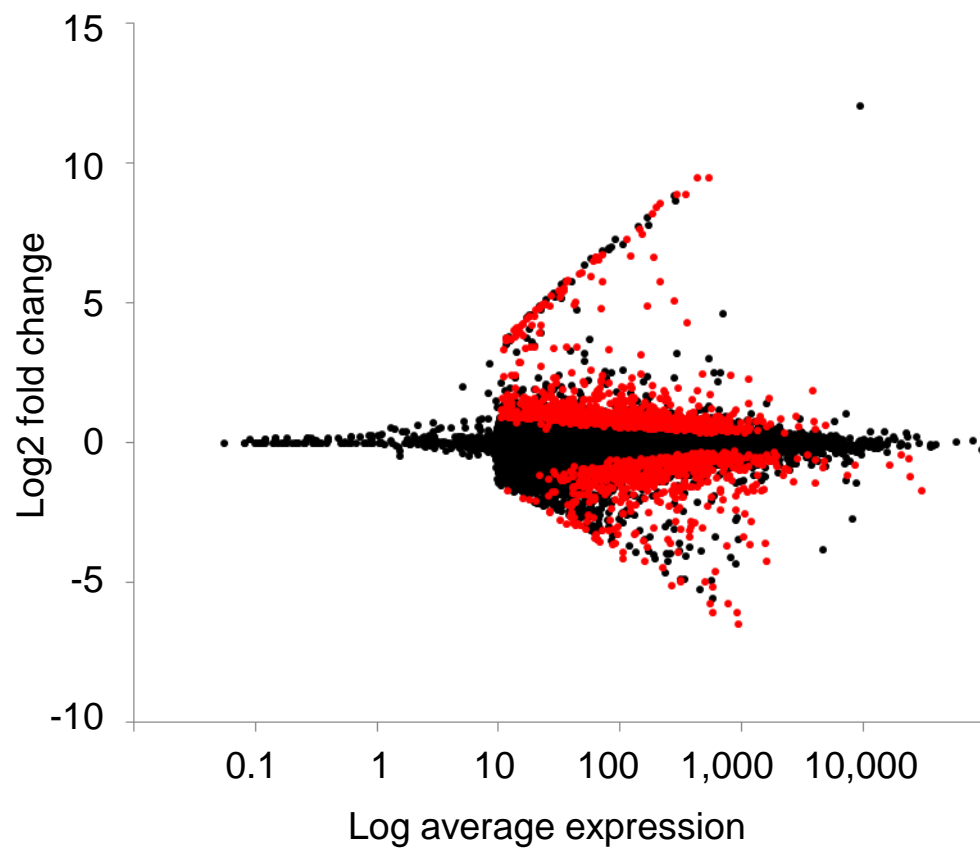
GO:0000155:phosphorelay sensor kinase activity, 13, 43, 2e-14 ↓↑
GO:0071805:potassium ion transmembrane transport, 28, 83, 2e-14 ↓↑

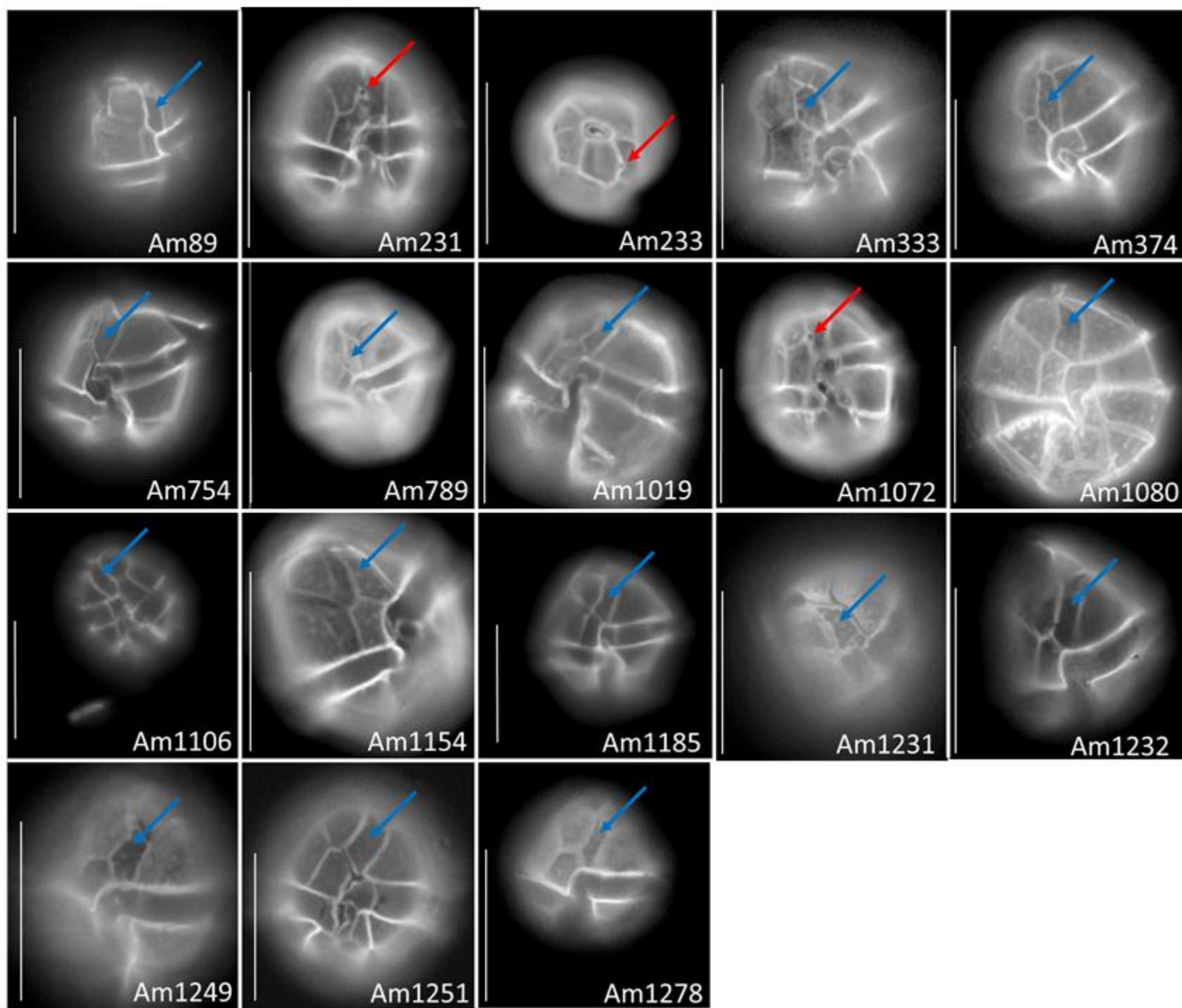
GO:0010467:gene expression, 18, 46, 2e-06 ↓↑
 GO:0007268:synaptic transmission, 24, 56, 3e-06 ↓↑
 GO:0004315:3-oxoacyl-[acyl-carrier-prot.] synthase activity, 19, 43, 8e-06 ↓↑
 GO:0005929:cilium, 28, 81, 1e-05 ↓↑
 GO:0016070:RNA metabolic process, 6, 26, 4e-05 ↓↑
GO:0008076:voltage-gated potassium channel complex, 13, 33, 9e-05 ↓↑

a



b





Supplementary Table 1: Results of model fitting for seven alternative models of divergence. *SI* is the strict isolation model. *IM* is the Isolation-with-Migration model, *AM* the Ancient Migration model, and *SC* is the Secondary Contact model. All three models of divergence-with-gene-flow were implemented using one, shared migration rate in each direction (m_{12} , m_{21}) across the genome (homogeneous migration), or with two categories of migration rates in each direction across the genome (heterogeneous migration).

Model	k	MLE	AIC	Δ_i	$L(\text{Mil}y)$	Theta	nu1	nu2	m12	m21	me12	me21	Ts	Tps	P
<i>SI</i>	4	-12154	24316	22172	0	110008	0.98	1.67	-	-	-	-	0.34	-	-
<i>IM</i>	6	-5974	11960	9816	0	48985	1.97	2.04	0.16	0.64	-	-	3.34	-	-
<i>AM</i>	7	-5971	11956	9812	0	41411	2.33	2.40	0.14	0.55	-	-	4.22	0,00	-
<i>SC</i>	7	-4372	8758	6614	0	78799	1.31	1.36	0.38	2.46	-	-	1.07	0.19	-
<i>IM2M</i>	9	-2082	4182	2038	0	41054	1.98	4.14	0.61	1.34	0.06	0.00	3.86	-	0,30
<i>AM2M</i>	10	-2112	4244	2100	0	39529	2.02	4.31	0.64	1.26	0.06	0.00	4.00	0.00	0.30
<i>SC2M</i>	10	-1062	2144	0	1	82530	0.8	2.3	6.09	6.01	0.26	0.00	0.94	0.10	0,43

k The number of free parameters in the model

MLE maximum likelihood estimate

AIC Akaike Information Criterion

Δ_i Difference in AIC between model *i* and the best model (*SC2M*)

$L(\text{Mil}y)$ Relative likelihood of model *i* compared to the best model (*SC2M*)

Theta Theta parameter for the ancestral population before split ($\theta = 2N_{\text{ref}}\mu$), with N_{ref} being the effective size of the ancestral population, and μ the per-site mutation rate per generation.

nu1 The effective size of the A species relative to N_{ref}

nu2 The effective size of the B species relative to N_{ref}

m12 The neutral movement of genes from the B to the A lineage in units of $N_{\text{ref}}m_{2>1}$ generations

m21 The neutral movement of genes from the A to the B lineage in units of $N_{\text{ref}}m_{1>2}$ generations

me12 The effective migration rate of “genomic-island” genes from the B to the A lineage

me21 The effective migration rate of “genomic-island” genes from the A to the B lineage

Ts The time of split in units of N_{ref} generations

Tps The time of migration stop (*AM* model) or start (*SC* model) post-split in units of N_{ref} generations

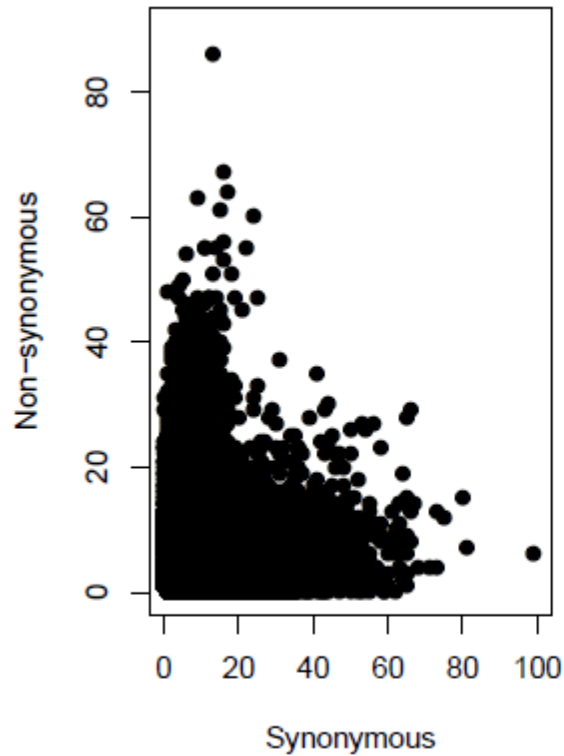
P The proportion of the SNPs experiencing reduced effective migration rate

Supplementary Table 2: Results of model fitting for seven alternative models of divergence, using a single randomly chosen SNP per transcript. A total of 5 different subsets were tested. Abbreviation as in Supplementary Table 1.

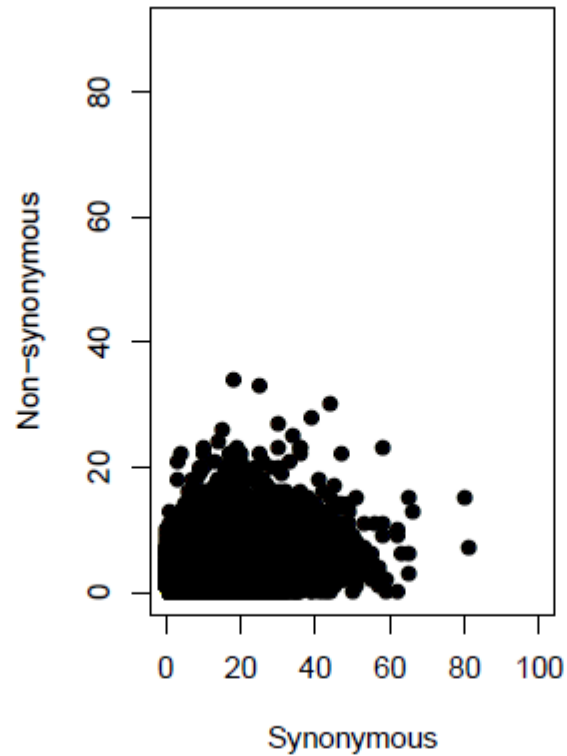
Subset	Model	k	MLE	Theta	nu1	nu2	m12	m21	me12	me21	Ts	Tps	P
1	SI	4	-1731	5054	0.11	0.31	-	-	-	-	0.03	-	-
	IM	6	-1222	6299	0.17	0.38	3.75	4.99	-	-	0.36	-	-
	IM2M	9	-1014	1265	0.73	3.62	2.37	0.97	0.05	0.02	6.28	-	0.90
	AM	7	-1339	1046	1.07	3.87	0.76	0.49	-	-	9.97	0.00	-
	AM2M	10	-1731	5050	0.12	0.32	0.06	0.00	0.00	0.00	0.00	0.03	0.00
	SC	7	-607	921	1.11	0.59	0.69	4.68	-	-	14.89	0.35	-
	SC2M	10	-379	728	0.91	1.39	1.55	7.98	0.09	0.00	17.85	0.23	0.95
2	SI	4	-1701	5058	0.12	0.38	-	-	-	-	0.03	-	-
	IM	6	-1181	14411	0.07	0.16	9.06	14.98	-	-	0.34	-	-
	IM2M	9	-989	1215	0.60	3.97	2.72	0.93	0.01	0.01	7.53	-	0.95
	AM	7	-1382	907	1.39	4.80	0.65	0.42	-	-	9.46	0.00	-
	AM2M	10	-1701	5061	0.12	0.38	0.00	0.00	0.00	0.00	0.00	0.03	0.00
	SC	7	-635	788	1.62	1.39	0.55	3.04	-	-	14.33	0.47	-
	SC2M	10	-288	431	1.01	1.11	1.20	7.25	0.46	0.00	36.84	0.28	0.97
3	SI	4	-1752	5076	0.10	0.32	-	-	-	-	0.03	-	-
	IM	6	-1352	4262	0.26	1.02	3.27	2.40	-	-	1.18	-	-
	IM2M	9	-1017	1214	0.54	3.87	2.96	0.79	0.01	0.01	7.77	-	0.96
	AM	7	-1507	914	1.87	3.81	0.43	0.50	-	-	9.95	0.01	-
	AM2M	10	-1752	5077	0.10	0.32	0.09	0.02	0.00	0.00	0.00	0.03	0.00
	SC	7	-643	570	1.20	0.69	0.70	4.53	-	-	29.91	0.46	-
	SC2M	10	-372	539	0.60	0.99	1.97	11.20	0.30	0.00	28.33	0.16	0.96
4	SI	4	-1620	5064	0.11	0.32	-	-	-	-	0.03	-	-
	IM	6	-1125	11891	0.08	0.19	7.97	12.40	-	-	0.35	-	-
	IM2M	9	-1066	966	1.44	3.68	1.01	0.62	0.01	0.01	8.85	-	0.92
	AM	7	-1202	1663	0.53	2.50	1.69	0.86	-	-	9.76	0.00	-
	AM2M	10	-1620	5063	0.11	0.32	0.00	0.00	0.00	0.00	0.00	0.03	0.00
	SC	7	-673	553	1.69	1.07	0.54	2.70	-	-	25.48	0.68	-
	SC2M	10	-498	903	0.86	2.90	2.51	9.32	0.10	0.00	11.28	0.17	0.97
5	SI	4	-1749	5126	0.10	0.34	-	-	-	-	0.03	-	-
	IM	6	-1186	9711	0.09	0.25	9.14	9.98	-	-	0.34	-	-
	IM2M	9	-1031	1265	0.52	3.86	2.65	0.77	0.01	0.01	7.64	-	0.96
	AM	7	-1319	1179	0.91	3.35	0.88	0.48	-	-	9.98	0.00	-
	AM2M	10	-1749	5117	0.11	0.36	0.22	0.37	0.00	0.00	0.00	0.03	0.05
	SC	7	-556	659	1.15	0.66	0.67	4.81	-	-	24.53	0.38	-
	SC2M	10	-329	551	0.60	0.99	1.96	11.37	0.30	0.00	28.82	0.17	0.96

Supplementary Material

a



b



c

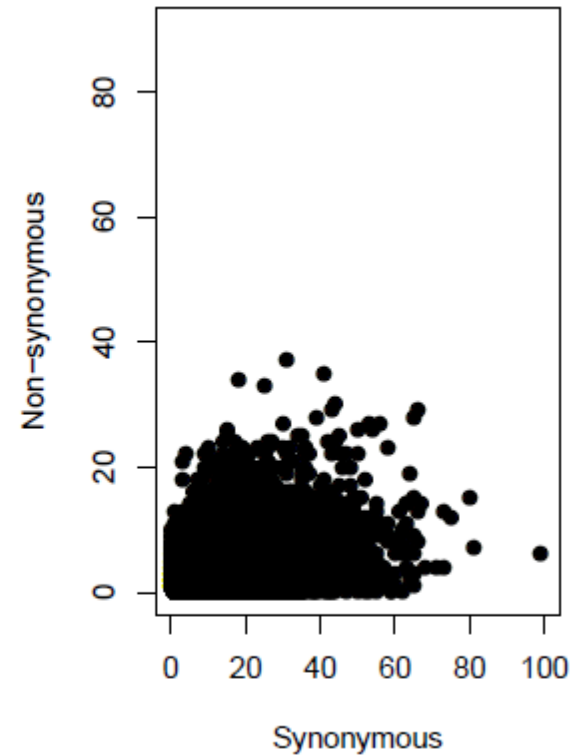


Fig. S1. Selecting the reading frame minimizing the proportion of non-synonymous mutations when several reading frames are possible. (A) considering all transcripts and all possible reading frames, (B) only considering transcripts with a single possible reading frame, (C) considering all transcript and the reading frame minimizing the number of non-synonymous mutations.